Nonlinear neoclassical transport in toroidal edge plasmas

T. Fülöp[a)]
Department of Electromagnetics, Chalmers University of Technology, Gothenburg 412 96, Sweden

P. Helander
UKAEA/Euratom Fusion Association, Culham Science Centre, Abingdon, Oxon, OX14 3DB, United Kingdom

(Received 18 December 2000; accepted 26 March 2001)

In conventional neoclassical theory, the density and temperature gradients are not allowed to be as steep as frequently observed in the tokamak edge. In this paper the theory of neoclassical transport in a collisional, impure plasma is extended to allow for steeper profiles than normally assumed. The dynamics of highly charged impurity ions then becomes nonlinear, which affects the transport of all species. As earlier found in the banana regime, when the bulk plasma gradients are large the impurity ions undergo a poloidal redistribution, which reduces their parallel friction with the bulk ions and suppresses the neoclassical ion particle flux. The neoclassical confinement is thus improved in regions with large radial gradients. When the plasma is collisional and the gradients are large, the impurities accumulate on the inboard side of the torus. © *2001 American Institute of Physics.* [DOI: 10.1063/1.1372179]

I. INTRODUCTION

From years of experiments on the world's premier tokamaks it is well known that the plasma edge has a decisive influence on tokamak performance. Numerical simulations of core plasma turbulence also suggest that the edge plasma plays an important role in regulating the overall confinement.[1] The present theoretical understanding of the edge plasma is, however, fairly incomplete. Not even its neoclassical transport properties can be predicted with any confidence, since the plasma profiles are frequently too steep for conventional neoclassical theory to be valid, especially in the H-mode pedestal region.

In this region, very strong poloidal impurity asymmetries have been observed in recent experiments in the Alcator C-Mod,[2,3] but the mechanism giving rise to these asymmetries and its implications for the transport are not known. One of the possible causes for the poloidal accumulation of the impurities is the strong ion-impurity friction caused by large radial density and temperature gradients in this region. (The parallel ion flow is proportional to these gradients.) If the parallel ion-impurity friction is large enough to compete with the parallel impurity pressure gradient, then the impurities are not able to move freely over the flux surface, and therefore accumulation of impurities will arise, as was shown recently in Refs. 4 and 5. However, these papers considered the case where the bulk plasma ions and electrons are nearly collisionless, while the edge collisionality in the Alcator C-Mod is much higher.

This has motivated the study presented in this paper, where the nonlinear neoclassical transport theory of Refs. 4 and 5 is extended to the Pfirsch–Schlüter (high-collisionality) regime. Nonlinear transport in this regime has been examined earlier in Ref. 6, but only for an isothermal plasma in a simplified geometry. We find that an up–down asymmetry is indeed expected for parameters typical of the plasma edge, and this asymmetry has the same qualitative features as those observed in the experiments. However, the measured effect is substantially larger than the theoretical prediction. As in the banana regime, the calculated poloidal impurity redistribution turns out to have interesting implications for the cross-field neoclassical transport. The neoclassical ion particle flux becomes nonlinear and nonmonotonic as a function of the local gradients, and the heat flux is also affected.

Conventional neoclassical theory[7–9] is based on the requirement that the expansion parameter $\delta \equiv \rho_\theta / L_\perp$ should be infinitesimally small, where ρ_θ is the poloidal ion gyroradius and $L_\perp$ the radial scale length associated with the density and temperature profiles. As the radial scale length decreases, poloidal asymmetries arise in the plasma.[10–12] In an impure plasma, typically the first plasma parameter to develop a poloidal variation is the impurity density, n_z,[6] whose poloidal modulation is of the order $\tilde{n}_z / n_z \sim \delta_z \equiv \delta \hat{\nu}_{ii} z^2$, where $\hat{\nu}_{ii} \equiv L_\parallel / \lambda_{ii}$ is the collisionality, with λ_{ii} the mean-free path for the bulk ions and $L_\parallel$ the connection length. In conventional neoclassical theory δ_z is assumed to be small. In this paper, we adopt the ordering $\delta \ll 1, \delta_z = O(1)$, which is more realistic for the tokamak edge.

Let us pause briefly to discuss the meaning of this ordering. As in all neoclassical theory, our basic expansion parameter is $\delta \ll 1$, while a *subsidiary* expansion is performed in the largeness of the collisionality parameter $\hat{\nu}_{ii}$. Allowing $\delta_z = \delta \hat{\nu}_{ii} z^2$ to be of order unity thus implies that $z = O(\delta^{-1/2})$ is formally regarded as large, so that we are limited to considering heavy impurities. It should be noted that δ_z is only assumed to be of order unity on the scale set by δ, and this does not preclude the possibility of δ_z being

a)Electronic mail: tunde@elmagn.chalmers.se

numerically larger than unity, as long as it does not become as large as z, for example.

Even stronger gradients were recently treated in Ref. 13, which considers Pfirsch–Schlüter transport in a collisional plasma without impurities and effectively adopts the ordering $\delta\hat{\nu}_{ii}=O(1)$, which would correspond to $\delta_z=O(z^2)$. Thus, while Ref. 13 considers gradients that are so steep that the parallel dynamics of the bulk ions becomes nonlinear, we are content with considering the case of weaker gradients where only heavy impurities are nonlinear. While even the parameter $\delta\hat{\nu}_{ii}$ is likely to approach unity in the pedestal regime, it is clear that the parameter δ_z becomes large long before $\delta\hat{\nu}_{ii}$ does, if heavy impurities are present. Thus the modifications to neoclassical theory presented in this paper are likely to be significant in the plasma edge where impurities are abundant.

The reason why we cannot allow δ_z to be as large as z^2 is that we choose to keep the aspect ratio ϵ^{-1} arbitrary. If $\delta_z=O(z^2)$ and $\epsilon=O(1)$, the *bulk* ion density begins to vary significantly over each surface, and the transport becomes mathematically intractable. The authors of Ref. 13 overcome this problem by instead expanding in $\epsilon\ll 1$. Another difficulty with treating very steep gradients is that the usual separation in time scales between parallel and perpendicular transport breaks down when δ_z becomes large enough. When this occurs, the precise condition for which was derived in Ref. 4, the transport cannot be analyzed on one flux surface at a time, and thus loses its local nature.

We also restrict our attention to the case of a hydrogen plasma (i) with a single species of highly charged ($z\gg 1$) impurity ions. Both these species are taken to be collisional, as is typically the case in the edge of high-density discharges. We evaluate the particle and heat fluxes in two opposite limits: that of trace impurities, $Z_{\mathrm{eff}}-1=n_z z^2/n_i\ll 1$, and the Lorentz limit $n_z z^2/n_i\gg 1$. In the first case the impurities do not affect the kinetics of the bulk plasma, while in the second case the frequency of ion-impurity collisions exceeds that of ion–ion collisions. The nonlinear behavior of the impurities turns out to be quite similar in these two limits.

The rest of the paper is organized as follows. Section II is devoted to the analysis of the parallel impurity dynamics and the derivation of the equation governing the poloidal impurity distribution in the limits of trace impurity and large impurity concentration, respectively. Furthermore, the effect of the ion electron heat-exchange is discussed in the trace impurity limit. In Sec. III the neoclassical particle and heat fluxes are calculated, and the conclusions are summarized in Sec. IV.

II. PARALLEL IMPURITY DYNAMICS

The poloidal impurity distribution is governed by the parallel momentum equation,

$$m_z n_z \mathbf{b}\cdot(\mathbf{V}_z\cdot\boldsymbol{\nabla}\mathbf{V}_z)+zn_z e\boldsymbol{\nabla}_\parallel\tilde{\Phi}+\boldsymbol{\nabla}_\parallel p_z+\mathbf{b}\cdot\boldsymbol{\nabla}\cdot\overleftrightarrow{\boldsymbol{\pi}}_z=R_{zi\parallel}, \tag{1}$$

where $\mathbf{b}=\mathbf{B}/B$, $\tilde{\Phi}$ is the electrostatic potential, $R_{zi\parallel}$ is the impurity-ion parallel friction force and $\overleftrightarrow{\boldsymbol{\pi}}_z$ is the viscosity. In Eq. (1) inertia and parallel viscosity can be neglected, being smaller than the parallel pressure gradient by the factor $\delta/(z\hat{\nu}_{ii})\ll 1$. As a consequence of strong ion-impurity temperature equilibration, the impurity pressure is equal to $p_z=n_z T_i$, where T_i is the bulk ion temperature, which is nearly constant on each flux surface; see Ref. 4. These simplifications reduce Eq. (1) to

$$zn_z e\boldsymbol{\nabla}_\parallel\tilde{\Phi}+T_i\boldsymbol{\nabla}_\parallel n_z=R_{zi\parallel}. \tag{2}$$

Since the impurities are highly charged, their perpendicular velocity is dominated by the **E×B** drift, $\mathbf{V}_{z\perp}\simeq\mathbf{b}\times\boldsymbol{\nabla}\Phi/B$. As the electrostatic potential is nearly constant on flux surfaces, $\Phi\simeq\Phi_0(\psi)$, which can be verified *a posteriori*, it follows from the impurity continuity equation, $\boldsymbol{\nabla}\cdot(n_z\mathbf{V}_z)=0$, that there is a parallel impurity return flow equal to

$$V_{z\parallel}=-\frac{I}{B}\frac{d\Phi_0}{d\psi}+\frac{K_z(\psi)B}{n_z}, \tag{3}$$

where $K_z(\psi)$ is an integration constant proportional to the poloidal flow velocity and $\mathbf{B}=I(\psi)\boldsymbol{\nabla}\varphi+\boldsymbol{\nabla}\varphi\times\boldsymbol{\nabla}\psi$ is the magnetic field, so that ψ is the poloidal flux.

The ion-impurity parallel friction force $R_{zi\parallel}$ can be calculated from

$$R_{zi\parallel}=-\int m_i v_\parallel C_{iz}(f_{i1})d^3v, \tag{4}$$

where the subscript on the ion distribution function f_i refers to the ordering in δ. In lowest order, the ion distribution function is Maxwellian and constant on flux surfaces, $f_{i0}=f_{i0}(\psi)$, so the next-order correction, f_{i1}, is needed to evaluate the friction. Since the mass ratio is large, $m_z/m_i\gg 1$, ion-impurity collisions are described by the operator $C_{iz}^l\simeq\nu_{iz}(\mathcal{L}+(m_i v_\parallel/T_i)V_{z\parallel}f_{i0})$, where ν_{iz} is the ion-impurity collision frequency, and the Lorentz scattering operator is defined as

$$\mathcal{L}=\frac{2v_\parallel}{v^2 B}\frac{\partial}{\partial\lambda}\lambda v_\parallel\frac{\partial}{\partial\lambda},$$

with $\lambda=v_\perp^2/(Bv^2)$. The expression for the friction force is thus simplified to

$$R_{zi\parallel}=\int m_i v_\parallel\nu_{iz}\left(f_{i1}-\frac{m_i v_\parallel}{T_i}V_{z\parallel}f_{i0}\right)d^3v. \tag{5}$$

Next, we need to determine the first-order ion distribution function f_{i1}, which then, from the parallel momentum equation, Eq. (1), enables us to derive an equation governing the poloidal density variation of impurities $n_z(\theta)$. The ion distribution function is governed by the drift kinetic equation,

$$v_\parallel\boldsymbol{\nabla}_\parallel f_{i1}+\mathbf{v}_D\cdot\boldsymbol{\nabla}f_{i0}+\frac{ev_\parallel}{T_i}\boldsymbol{\nabla}_\parallel\tilde{\Phi}f_{i1}=C_{ii}(f_{i1})+C_{iz}(f_{i1}), \tag{6}$$

which, in the Pfirsch–Schlüter regime, is solved by an expansion in the mean-free path parameter $\Delta\equiv\hat{\nu}_{ii}^{-1}$, following Hazeltine.[14] Here, $\mathbf{v}_D=-v_\parallel\mathbf{b}\times\boldsymbol{\nabla}(v_\parallel/\Omega_i)$ is the drift velocity and $\Omega_i=eB/m_i$ is the gyrofrequency of the bulk ions.

Before solving this equation, which is done separately in the next three subsections in the limits of small and large impurity concentration, it is useful to inspect its moments. As in Ref. 14, the number and energy moments imply that the parallel particle and heat fluxes must be of the form

$$n_i V_{i\|} = -\frac{I p_i}{eB}\left(\frac{d\ln p_i}{d\psi} + \frac{e}{T_i}\frac{d\Phi}{d\psi}\right) + K_i(\psi)B, \tag{7}$$

and

$$q_{i\|} = -\frac{5 I p_i}{2eB}\frac{dT_i}{d\psi} + L_i(\psi)B, \tag{8}$$

where the integration constants $K_i(\psi)$ and $L_i(\psi)$ are flux functions. In the expression for the heat flux we have assumed that the energy exchange between ions and electrons can be neglected. In Sec. II B we analyze the consequences of finite ion–electron energy exchange. Energy exchange between the bulk and impurity ions can be neglected in the ordering we have adopted.

A. Trace impurities in a collisional plasma

We first consider the limit $n_z z^2/n_i \ll 1$, in which the impurities do not affect the parallel kinetics of the background ions. The background-ion distribution function can therefore be obtained by solving the drift-kinetic equation,

$$v_\| \nabla_\| f_i + \mathbf{v}_D\cdot\nabla f_i + \frac{e v_\|}{T_i}\nabla_\|\tilde{\Phi} f_i = C_{ii}(f_i), \tag{9}$$

where we have neglected ion-impurity collisions, being less frequent than ion–ion collisions by the factor $n_z z^2/n_i \ll 1$. To order $(\delta^1\Delta^{-1})$ we have $C_{ii}(f_{i1}^{-1})=0$, which implies

$$f_{i1}^{-1} = \left(\frac{\tilde{p}_i}{p_i} + \frac{m_i v_\| \tilde{V}_{i\|}}{T_i} + \frac{\tilde{T}_i}{T_i}\left(x^2 - \frac{5}{2}\right)\right) f_{i0}, \tag{10}$$

where the subscript and superscript on f_i refer to the orderings in δ and Δ, respectively, $x = v/v_{Ti}$ with $v_{Ti} = (2T_i/m_i)^{1/2}$, and the notation $\tilde{p}_i = p_{i1}^{-1}, \tilde{T}_i = T_{i1}^{-1}, \tilde{V}_{i\|} = V_{i\|1}^{-1}$ is used for simplicity.

To order $(\delta^1\Delta^0)$ we obtain

$$C_{ii}(f_{i1}^0) = v_\|\nabla_\| f_{i1}^{-1} + \frac{e v_\|}{T_i}\nabla_\|\tilde{\Phi} f_{i0}, \tag{11}$$

which, by multiplying by $m_i v_\|$ and integrating over velocity space, gives

$$\nabla_\|\tilde{p}_i + n_i e \nabla_\|\tilde{\Phi} = 0. \tag{12}$$

It follows from Eq. (7) that $\tilde{V}_{i\|} = \tilde{K}_i(\psi)B/n_i$, where $\tilde{K}_i(\psi)$ is an integration constant determining the poloidal rotation of the plasma. Using Eqs. (12) and (7) then simplifies Eq. (11) to

$$C_{ii}(f_{i1}^0) = v_\|\left(x^2 - \frac{5}{2}\right)\frac{\nabla_\|\tilde{T}_i}{T_i} f_{i0} + \frac{m_i v^2}{T_i} P_2(\xi)\tilde{K}_i(\psi)\nabla_\|\ln B f_{i0}, \tag{13}$$

where $P_2(\xi) = (3\xi^2 - 1)/2$ and $\xi = v_\|/v$. Furthermore, we note that the flux-surface average of the $m_i v_\| B$-moment of Eq. (9) gives

$$\langle (p_{i\|} - p_{i\perp})\nabla_\| B + n_i e B \nabla_\|\tilde{\Phi}\rangle = 0, \tag{14}$$

where $\langle\cdots\rangle$ denotes flux-surface averaging. Since $\tilde{n}_i/n_i$ and $e\tilde{\Phi}/T_i$ are both of order $\delta\Delta^{-1}$, the second term is $O(\delta^2)$ and

$$\langle (p_{i\|} - p_{i\perp})\nabla_\| B\rangle = 0 \tag{15}$$

holds to $O(\delta)$, leading to the conclusion that the $P_2(\xi)$ component of f_{i1}^0 has to vanish. Since this component is proportional to $\tilde{K}_i(\psi)$, see Eq. (13), it then follows that $\tilde{K}_i(\psi)=0$ and we thus have

$$C_{ii}(f_{i1}^0) = v_\|\left(x^2 - \frac{5}{2}\right)\frac{\nabla_\|\tilde{T}_i}{T_i} f_{i0}. \tag{16}$$

Solving this Spitzer problem as in Ref. 14 gives

$$f_{i1}^0 = f_{\rm hom} + f_{\rm part}, \tag{17}$$

where the homogeneous solution represents a Maxwellian perturbation,

$$f_{\rm hom} = \left(\frac{\tilde{p}_i}{p_i} + \frac{m_i v_\| V_{i\|}}{T_i} + \frac{\tilde{T}_i}{T_i}\left(x^2 - \frac{5}{2}\right)\right) f_{i0}, \tag{18}$$

while the particular solution,

$$f_{\rm part} = -\frac{5}{48}\frac{\tau_i \nabla_\|\tilde{T}_i}{T_i}(2x^4 + x^2 - 20) v_\| f_{i0}, \tag{19}$$

where the ion collision time is defined as $\tau_i = 12\pi^{3/2}\epsilon_0^2 m_i^{1/2} T_i^{3/2}/n_i e^4 \ln\Lambda$, carries the heat flux,

$$q_{i\|} = -\frac{125}{32}\frac{n_i T_i \tau_i}{m_i}\nabla_\| T_i. \tag{20}$$

Combining this equation with Eq. (8) gives

$$\nabla_\| T_i = \frac{16}{25}\frac{I T_i}{\Omega_i \tau_i}\frac{d\ln T_i}{d\psi}(1 - b^2), \tag{21}$$

where the magnetic field strength has been normalized so that $b \equiv B/\langle B^2\rangle^{1/2}$.

Inserting the results (17), (18) and (19) in Eq. (5) gives

$$R_{z i\|} = \frac{m_i n_i}{\tau_{iz}}\left(V_{i\|} - V_{z\|} + \frac{25}{16}\frac{\tau_i \nabla_\| T_i}{m_i}\right), \tag{22}$$

where $\tau_{iz} = (n_i/\sqrt{2} n_z z^2)\tau_i$, so that $\nu_{iz} = 3\pi^{1/2}/4\tau_{iz}x^3$. The parallel velocity $V_{i\|}$ of the bulk ions can be determined by calculating the parallel viscosity associated with f_{i1}^1, which is obtained by going to the next order in Δ. This calculation is presented in Ref. 14 and leads to the result

$$V_{i\|} - V_{z\|} = -\frac{I T_i}{m_i \Omega_i}\left(\frac{d\ln p_i}{d\psi} + \frac{d\ln T_i}{d\psi} \times\left(1.8 b^2 + 0.05\frac{b^2\langle(\nabla_\|\ln b)^2\rangle}{\langle(\nabla_\| b)^2\rangle}\right)\right) - \frac{K_z B}{n_z}, \tag{23}$$

which is not affected by the presence of trace impurities. Also, Eq. (22) agrees with the corresponding expression in

Ref. 9. The only differences between the present case and the conventional theory of Pfirsch–Schlüter transport in an impure plasma is that the impurity density n_z varies over the flux surface and the poloidal impurity rotation K_z is different, as we shall see shortly.

Returning to the parallel momentum equation (2) that governs the poloidal impurity distribution, we note that Eq. (21) implies that the ion temperature indeed varies less over the flux surface than the magnetic field strength, as assumed in Eq. (2). The poloidal electric field, $-\nabla_\parallel\tilde{\Phi}$, in Eq. (2) is determined by quasineutrality,

$$zn_z e\nabla_\parallel\tilde{\Phi}=-\frac{zn_zT_e}{T_e+T_i}\nabla_\parallel T_i$$

$$=-\frac{16}{25z\sqrt{2}}\frac{T_e}{T_e+T_i}\frac{Ip_i}{\Omega_i\tau_{iz}}\frac{d\ln T_i}{d\psi}(1-b^2), \qquad (24)$$

and is $O(z^{-1})$ smaller than the friction force. Using these results in Eq. (2) then gives

$$\frac{\partial n}{\partial\vartheta}=-\frac{m_in_iI}{e\tau_{iz}n_z\langle\mathbf{B}\cdot\nabla\theta\rangle}\left\{n\left(\frac{d\ln p_i}{d\psi}-\frac{d\ln T_i}{d\psi}\right)\right.$$

$$\left.+2.8nb^2\frac{d\ln T_i}{d\psi}+\frac{eB^2}{I\langle n_z\rangle T_i}K_z\right\}, \qquad (25)$$

where the impurity density and the poloidal angle have been normalized, $n=n_z/\langle n_z\rangle$ and $d\vartheta/d\theta\equiv\langle\mathbf{B}\cdot\nabla\theta\rangle/\mathbf{B}\cdot\nabla\theta$, and the term involving the small coefficient 0.05 in Eq. (23) has been neglected. Integrating Eq. (25) over ϑ allows us to determine the poloidal impurity flow,

$$K_z=-\frac{I\langle n_z\rangle T_i}{\langle B^2\rangle e}\left(\frac{d\ln n_i}{d\psi}+2.8\langle nb^2\rangle\frac{d\ln T_i}{d\psi}\right), \qquad (26)$$

and the equation for the poloidal distribution of the normalized impurity density thus finally becomes

$$\frac{\partial n}{\partial\vartheta}=g(n-b^2+\gamma(n-\langle nb^2\rangle)b^2). \qquad (27)$$

Here $\gamma=2.8(\ln T_i)'/(\ln n_i)'$ is a constant, the prime denotes a derivative with respect to ψ and

$$g=-\frac{m_in_iI}{e\tau_{iz}n_z\langle\mathbf{B}\cdot\nabla\theta\rangle}\left(\frac{d\ln p_i}{d\psi}-\frac{d\ln T_i}{d\psi}\right)=O(\delta_z)$$

measures the steepness of the bulk ion density and temperature profiles.

Equation (27) has exactly the same form as was found in the mixed-collisionality regime,[4] where the bulk ions and electrons are collisionless and the impurities collisional. Only the constants g and γ are different. As in that regime, the impurities accumulate on the inboard side of the tokamak when the gradients are steep, $g\lesssim 1$, thereby reducing the impurity-ion parallel friction. Indeed, in the limit when the pressure or temperature gradients are so large that $g\gg 1$ we can expand the solution of Eq. (27) in g^{-1}: $n=n_0+n_1+O(g^{-2})$, giving the following expression to lowest order:

$$n_0=\frac{\gamma}{1-\langle(1+\gamma b^2)^{-1}\rangle}\frac{b^2}{1+\gamma b^2}, \qquad (28)$$

which indicates that the impurities are pushed toward the inboard side of the torus where b is large. Conventional neoclassical theory assumes $g\ll 1$ and therefore neglects these effects.

B. Ion–electron heat exchange

If the collisionality is high, ion–electron energy transfer may influence the ion dynamics, as pointed out by Engelmann and Nocentini.[10] Starting from the ion drift kinetic equation and expanding in the usual way in the smallness of the mean-free path, we can include the ion–electron energy transfer by treating C_{ie}/C_{ii} as $O(\Delta)$. Then, to lowest order we have

$$C_{ii}(f_{i1}^{-1})=0, \qquad (29)$$

and to first order we have

$$v_\parallel\nabla_\parallel f_{i1}^{-1}+\frac{ev_\parallel}{T_i}\nabla_\parallel\tilde{\Phi}=C_{ii}(f_{i1}^0)+C_{ie}(f_{i1}^{-1}), \qquad (30)$$

instead of Eq. (11). Since $C_{ie}(f_{i1}^{-1})$ is even in $v_\parallel$, the odd part of f_{i1}^0 is given by

$$f_{i1}^0|_{\rm odd}=-\frac{v_\parallel I}{15\Omega_i}\frac{d\ln T_i}{d\psi}(1-b^2)(2x^4+x^2-20)f_{i0}$$

$$+\frac{m_iv_\parallel V_{i\parallel}}{T_i}f_{i0}, \qquad (31)$$

as obtained in conventional theory, see Eq. (19). The $(m_iv^2/2-5T_i/2)$ moment of the drift kinetic equation becomes

$$\nabla_\parallel\left(\frac{\chi_\parallel}{B}\nabla_\parallel\tilde{T}_i-\frac{5Ip_i}{2eB^2}\frac{dT_i}{d\psi}\right)=\frac{3m_e}{m_i\tau_{ei}B}(T_i-T_e), \qquad (32)$$

where $\chi_\parallel=3.9T_i\tau_i/m_i$ is the heat conductivity corresponding to Eq. (20). Since the corresponding conductivity for electrons is higher by a square root of the mass ratio m_i/m_e, the electron temperature T_e on the right of Eq. (32) is practically constant over the flux surface. For consistency, T_e must be equal to the flux-surface average of the ion temperature, as follows from the average of Eq. (32) unless an ion heat source (or sink) is also included in this equation. To solve the equation explicitly, it is necessary to know the magnetic equilibrium. If the right-hand side is neglected one obtains the usual Pfirsch–Schlüter solution (21), while if the coefficient on the right hand side is large, then $\tilde{T}_i$ is small and the energy transport is suppressed.

For a standard, circular, large-aspect-ratio equilibrium Eq. (32) becomes

$$\frac{\partial}{\partial\theta}\left(\frac{\chi_\parallel}{qRB}\frac{\partial\tilde{T}_i}{\partial\theta}-\frac{5Ip_i}{2e\langle B\rangle^2}(1-2\epsilon\cos\theta)\frac{\partial T_i}{\partial\psi}\right)=\frac{3m_e}{m_i\tau_{ei}}\frac{qR}{B}\tilde{T}_i, \qquad (33)$$

with the result

$$\tilde{T}_i = -\frac{(5Ip_i/eB_0^2)(dT_i/d\psi)}{(\chi_\parallel/qRB)+(3m_eqR/m_i\tau_{ei}B)}\epsilon\sin\theta, \tag{34}$$

and it is clear that $\tilde{T}_i$ is simply reduced by a constant factor,

$$\mu = 1+\frac{3m_e}{m_i}\frac{q^2R^2}{\chi_\parallel\tau_{ei}} \simeq 1+\left(\frac{R}{\lambda_i}\right)^2\left(\frac{m_e}{m_i}\right)^{1/2}\left(\frac{T_i}{T_e}\right)^{3/2}, \tag{35}$$

where $\lambda_i = v_{Ti}\tau_i$. Thus the ion–electron heat exchange has a negligible effect on the plasma transport unless $R/\lambda_i \gtrsim (m_i/m_e)^{1/4}(T_e/T_i)^{3/4}$.

Unless $\mu - 1 \ll 1$, the poloidal distribution of impurities will be affected, since $\nabla_\parallel T_i$ is reduced by the factor μ, which in turn affects the controlling parameters g and γ of Eq. (27) in the following way:

$$g = -\frac{m_in_iI}{e\tau_{iz}n_z\langle \mathbf{B}\cdot\nabla\theta\rangle}\left(\frac{d\ln p_i}{d\psi}-\frac{1}{\mu}\frac{d\ln T_i}{d\psi}\right) \tag{36}$$

and

$$\gamma = \frac{(1.8+1/\mu)\ln T_i'}{\ln p_i' - (\ln T_i')/\mu}. \tag{37}$$

In the tokamak edge, the density profile is typically about twice as steep as the temperature profile, and it appears that the effect of ion–electron energy exchange does not affect the impurity dynamics very much. Even if $\mu\to\infty$, so that the parameter g grows by a half and γ falls to about a half compared to the case when $\mu = 1$, this has no dramatic effect on the impurities. The numerical solution of (27) shows that, as γ is reduced, the magnitude of the in–out asymmetry grows. As we shall see in the next section, this in–out asymmetry is associated with reduced neoclassical transport, and this effect is thus somewhat enhanced in the very high collisionality regime where ion-electron energy equilibration occurs.

C. Lorentz limit: $Z_{\text{eff}} \gg 1$

In the Lorentz limit $n_zz^2/n_i \gg 1$, impurity–ion collisions are more frequent than ion–ion collisions, $C_{ii} \ll C_{iz}$, and therefore significantly affect the bulk ion flow. The solution of the drift-kinetic equation,

$$v_\parallel\nabla_\parallel f_i + \mathbf{v}_D\cdot\nabla f_i = C_{ii}(f_i)+C_{iz}(f_i) \simeq C_{iz}(f_i), \tag{38}$$

is then the same as Eq. (10) in the order $\delta\Delta^{-1}$, but in the order $\delta^1\Delta^0$ we obtain

$$v_\parallel\nabla_\parallel f_{i1}^{-1} + \frac{ev_\parallel\nabla_\parallel\tilde{\Phi}}{T_i}f_{i0} = \nu_{iz}\left(\mathcal{L}(f_{i1}^0)+\frac{m_iv_\parallel}{T_i}V_{z\parallel}f_{i0}\right). \tag{39}$$

The solution of Eq. (39) can be written as

$$f_{i1}^0 \simeq \frac{m_iv_\parallel}{T_i}V_{z\parallel}f_{i0} - \frac{4\tau_{iz}}{3\sqrt{\pi}}v_\parallel \times x^3\left[\frac{\nabla_\parallel\tilde{p}_i}{p_i}+\frac{e\nabla_\parallel\tilde{\Phi}}{T_i}+\left(x^2-\frac{5}{2}\right)\frac{\nabla_\parallel\tilde{T}_i}{T_i}\right]f_{i0}. \tag{40}$$

Using parallel ion momentum conservation, the ion-impurity friction force can be written as

$$R_{zi\parallel} = -(\nabla_\parallel\tilde{p}_i + n_ie\nabla_\parallel\tilde{\Phi}), \tag{41}$$

where we need to express the parallel gradients as functions of radial gradients.

The particle and heat fluxes associated with f_{i1}^0 are

$$\begin{pmatrix} n_iV_{i\parallel}\\ q_{i\parallel}/T_i\end{pmatrix} = \int v_\parallel\begin{pmatrix}1\\ x^2-5/2\end{pmatrix}f_{i1}^0\,d^3v, \tag{42}$$

giving

$$\begin{pmatrix} n_i(V_{i\parallel}-V_{z\parallel})\\ q_{i\parallel}/T_i\end{pmatrix} = -\frac{p_i\tau_{iz}}{m_i}\begin{pmatrix}l_{11}&l_{12}\\ l_{21}&l_{22}\end{pmatrix}\begin{pmatrix}a_1\\ a_2\end{pmatrix}, \tag{43}$$

with

$$\begin{pmatrix}l_{11}&l_{12}\\ l_{21}&l_{22}\end{pmatrix} = \frac{1}{\pi}\begin{pmatrix}32/3&16\\ 16&200/3\end{pmatrix}, \tag{44}$$

and where $a_1 = \nabla_\parallel\tilde{p}_i/p_i + e\nabla_\parallel\tilde{\Phi}/T_i$ and $a_2 = \nabla_\parallel\tilde{T}_i/T_i$ are the usual thermodynamic forces.

Combining Eqs. (7) and (3) gives

$$\langle Bnn_i(V_{i\parallel}-V_{z\parallel})\rangle = 0 = -\frac{Ip_i}{e}\frac{d\ln p_i}{d\psi} + \left\langle\left(K_i-\frac{K_zn_i}{n_z}\right)nB^2\right\rangle, \tag{45}$$

which determines $K_i(\psi)$:

$$K_i(\psi)\langle nB^2\rangle - \frac{K_zn_i}{\langle n_z\rangle} = \frac{Ip_i}{e}\frac{d\ln p_i}{d\psi}, \tag{46}$$

so that

$$n_i(V_{i\parallel}-V_{z\parallel}) = -\frac{Ip_i}{eB}\frac{d\ln p_i}{d\psi}\left(1-\frac{b^2}{\langle nb^2\rangle}\right) + \frac{K_zBn_i}{\langle n_z\rangle}\left(\frac{1}{\langle nb^2\rangle}-\frac{1}{n}\right). \tag{47}$$

From Eq. (43) it follows that $\langle Bnq_{i\parallel}\rangle = 0$, and using Eq. (8), we can determine $L_i(\psi)$:

$$L_i(\psi)\langle nB^2\rangle = \frac{5I}{2e}\frac{dT_i}{d\psi}, \tag{48}$$

so that the parallel heat flux becomes

$$q_{i\parallel} = -\frac{5Ip_i}{2eB}\frac{dT_i}{d\psi}\left(1-\frac{b^2}{\langle nb^2\rangle}\right). \tag{49}$$

Using Eqs. (43), (47) and (49) we can express the thermodynamic forces as

$$\begin{pmatrix} a_1 \\ a_2 \end{pmatrix} = -\frac{m_i}{p_i \tau_{iz}} \begin{pmatrix} l_{11} & l_{12} \\ l_{21} & l_{22} \end{pmatrix}^{-1} \begin{pmatrix} n_i (V_{i\|} - V_{z\|}) \\ q_{i\|}/T_i \end{pmatrix}, \tag{50}$$

so that $a_2 = \nabla_\| \tilde{T}_i / T_i$ can be written as a function of the radial gradients:

$$\frac{\nabla_\| \tilde{T}_i}{T_i} = \frac{9\pi}{256} \left[-\frac{I}{\Omega_i \tau_{iz}} \left(\frac{d \ln n_i}{d\psi} - \frac{2}{3} \frac{d \ln T_i}{d\psi} \right) \times \left(1 - \frac{b^2}{\langle n b^2 \rangle} \right) + \frac{K_z B m_i}{T_i \tau_{iz} \langle n_z \rangle} \left(\frac{1}{\langle n b^2 \rangle} - \frac{1}{n} \right) \right]. \tag{51}$$

The ion-impurity friction force is

$$R_{zi\|} = -p_i a_1 = \frac{3\pi}{32} \left[\frac{m_i n_i}{\tau_{iz}} (V_{i\|} - V_{z\|}) + \frac{16}{\pi} n_i \nabla_\| \tilde{T}_i \right], \tag{52}$$

so using Eqs. (50) and (51) we arrive at

$$R_{zi\|} = -\frac{75\pi}{512} \frac{m_i n_i}{\tau_{iz}} \left[\frac{I T_i}{eB} \left(1 - \frac{b^2}{\langle n b^2 \rangle} \right) \left(\frac{d \ln p_i}{d\psi} - \frac{3}{5} \frac{d \ln T_i}{d\psi} \right) - \frac{K_z B}{\langle n_z \rangle} \left(\frac{1}{\langle n b^2 \rangle} - \frac{1}{n} \right) \right]. \tag{53}$$

The remaining unknown quantity K_z governs the poloidal impurity rotation and is determined from the parallel viscosity constraint,

$$\langle \mathbf{B} \cdot \nabla \cdot \overleftrightarrow{\pi} \rangle \simeq \left\langle (\nabla_\| B) \int m v^2 P_2(\xi) f_{i1}^1 \, d^3 v \right\rangle = 0, \tag{54}$$

where $P_2(\xi)$ denotes the Legendre polynomial $P_2(\xi) = (3\xi^2 - 1)/2$, with $\overleftrightarrow{\pi} = \overleftrightarrow{\pi}_i + \overleftrightarrow{\pi}_z$. The impurity viscosity is unimportant, since

$$\frac{\pi_{z\|}}{\pi_{i\|}} \sim \frac{n_i \tau_{zz}}{n_z \tau_{iz}} \sim \frac{n_z}{n_i} z^{-3/2} \ll 1, \tag{55}$$

which simplifies the calculation. The P_2 component of f_{i1}^1 is obtained from the next order in Δ of the kinetic equation,

$$v_\| \nabla_\| f_{i1}^0 + \mathbf{v}_D \cdot \nabla f_{i0} = C_i(f_{i1}^1) = \nu_{iz} \mathcal{L}(f_{i1}^1). \tag{56}$$

Using $\mathcal{L}(f_{i1}^1)|_{P_2} = -3 f_{i1}^1|_{P_2}$, where $(\cdots)|_{P_2}$ denotes the P_2-component of $(\cdots)$, Eq. (56) gives for this component

$$f_{i1}^1|P_2 = -\frac{v^2}{9} P_2(\xi) f_{i0} \left[-\frac{I}{\Omega_i} \left(\frac{d \ln p_i}{d\psi} + (x^2 - 5/2) \frac{d \ln T_i}{d\psi} \right) \times \nabla_\| \ln B - \frac{4 \tau_{iz} n_z}{3\sqrt{\pi}} x^3 \left((a_1 + (x^2 - 5/2) a_2) \frac{\nabla_\| \ln B}{n_z} + 2 \nabla_\| \left(\frac{a_1 + (x^2 - 5/2) a_2}{n_z} \right) \right) + \frac{m_i K_z}{T_i} \left(\frac{B}{n_z} \nabla_\| \ln B + 2 \nabla_\| \left(\frac{B}{n_z} \right) \right) \right]. \tag{57}$$

Employing this result in the parallel viscosity constraint (54) then gives the following expression for the poloidal impurity flow,

$$K_z = -\frac{I \langle n_z \rangle T_i}{\langle B^2 \rangle e} \left(\frac{d \ln p_i}{d\psi} + \frac{d \ln T_i}{d\psi} \right). \tag{58}$$

Finally, inserting these results in Eq. (2) and using quasineutrality, $n_e = n_i + z n_z$, gives the equation for the poloidal impurity distribution,

$$(1 + \alpha n) \frac{\partial n}{\partial \vartheta} = \hat{g} \left[n \left(1 + \frac{\hat{\gamma} - 1}{\langle n b^2 \rangle} b^2 \right) - \hat{\gamma} b^2 \right], \tag{59}$$

where $\alpha \equiv \langle Z_{\rm eff} - 1 \rangle T_e / (T_e + T_i) \gg 1$, $\hat{\gamma} = ((\ln p_i)' + (\ln T_i)') / ((\ln p_i)' - (3/5)(\ln T_i)')$ and

$$\hat{g} = -\frac{75\pi}{512} \frac{m_i n_i I}{e \tau_{iz} n_z \langle \mathbf{B} \cdot \nabla \theta \rangle} \left(\frac{d \ln p_i}{d\psi} - \frac{3}{5} \frac{d \ln T_i}{d\psi} \right) = O(\delta_z).$$

When the gradients become very large so that $\hat{g} \gg 1$, the square bracket on the right-hand side of Eq. (59) must vanish, so that the impurity distribution becomes

$$n \simeq \frac{\hat{\gamma} b^2}{1 + (\hat{\gamma} - 1/\langle n b^2 \rangle) b^2}, \tag{60}$$

which implies that the impurities again accumulate on the *inboard* side of the flux surface. This is the same basic behavior that we found in the limit of trace impurities at the end of Sec. II A, and in the banana regime investigated in Refs. 4 and 5.

D. Poloidal impurity distribution

The equations governing the poloidal distribution of impurities over each flux surface are given by Eqs. (27) and (59) in the limits of small and large impurity concentration, respectively. These equations are complicated integro-differential equations that are not amenable to analytical solution except in certain simple limits. One such limit is that of very steep radial plasma profiles, where the solutions are given by (28) and (60) and predict the accumulation of impurity ions on the inboard side of the torus. Another tractable

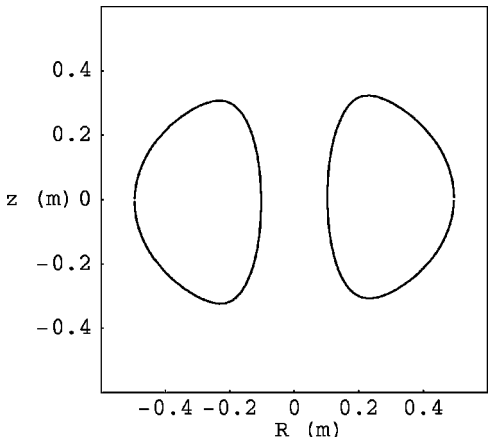

FIG. 1. Magnetic reconstruction of a flux surface close to the edge in START.

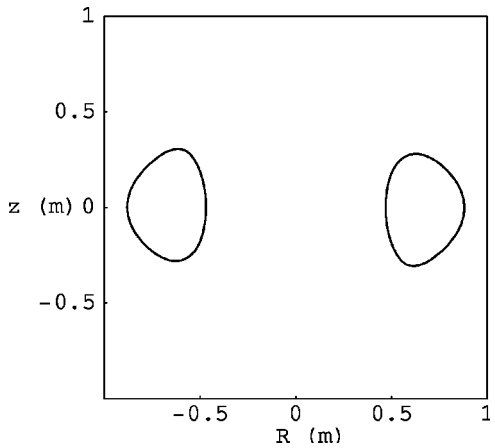

FIG. 2. Flux surface close to the edge ($r/a=0.9$) in the Alcator C-Mod.

limit is that of a large aspect ratio and circular cross section, in which case Eqs. (27) and (59) can be solved by making the expansions $b^2=1-2\epsilon\cos\theta+O(\epsilon^2)$, $n=1+n_c\cos\theta+n_s\sin\theta+O(\epsilon^2)$. The solutions then become

$$n_s=\frac{2\epsilon g}{1+(1+\gamma)^2g^2}, \tag{61}$$

$$n_c=-\frac{2\epsilon(1+\gamma)g^2}{1+(1+\gamma)^2g^2}, \tag{62}$$

in the limit of trace impurities, $\alpha\ll 1$, and in the Lorentz limit

$$n_s=\frac{2\epsilon g'}{1+(\hat{\gamma}-1)^2g'^2}, \tag{63}$$

$$n_c=-\frac{2\epsilon(\hat{\gamma}-1)g^2}{1+(\hat{\gamma}-1)^2g'^2}, \tag{64}$$

where $g'=\hat{g}/(1+\alpha)$. These expressions indicate that as the gradients represented by g and $\hat{g}$ are made successively larger, the impurities first develop an up–down asymmetry proportional to ϵg or $\epsilon\hat{g}$ and then an in–out asymmetry proportional to ϵ. This agrees completely with the behavior found for the banana regime in Refs. 4 and 5.

In the general case, Eqs. (27) and (59) must be solved by numerical means. We have done so for typical equilibria in two tokamaks: the Small Tight-Aspect-Ratio Tokamak (START)[15] and the Alcator C-Mod, for which magnetic reconstructions of magnetic surfaces in the edge are shown in Figs. 1 and 2. The results are shown in Figs. 3–4, and confirm the qualitative behavior expressed by the analytical solutions. An up–down asymmetry forms when the radial gradients are moderate, $g=O(1)$, and turns into an in-out asymmetry for larger gradients, $g\gg 1$, irrespective of the impurity concentration. In the Alcator C-Mod, an up–down asymmetry is indeed observed in the line radiation from heavy impurities near the plasma edge. Qualitatively, these observations agree with our predictions: the asymmetry has the correct sign and is reversed if the toroidal magnetic field is reversed. However, the observed asymmetries are much larger than those calculated here. This may be due to the fact that the parameter g is extremely large in these experiments while we have formally treated it as $O(1)$. A more extreme ordering, e.g., $g=O(z)\gg 1$, may describe the Alcator C-Mod experiments better.

III. NEOCLASSICAL TRANSPORT

We now proceed to evaluate the classical and neoclassical particle fluxes of the bulk ions,

$$\langle(\mathbf{\Gamma}_i^{\rm cl}+\mathbf{\Gamma}_i^{\rm neo})\cdot\nabla\psi\rangle=\left\langle\frac{R^2\,\nabla\varphi\cdot(\mathbf{R}_{iz_\perp}+\mathbf{R}_{iz\|})}{eB}\right\rangle.$$

Using the friction force $R_{zi\|}$ from Eq. (4) we obtain the average neoclassical particle flux across a flux surface,

$$\langle\mathbf{\Gamma}_i^{\rm neo}\cdot\nabla\psi\rangle=\frac{I\langle p_z\rangle\langle\mathbf{B}\cdot\nabla\theta\rangle}{e\langle B^2\rangle}\left\langle\frac{(1+\alpha n)}{b^2}\frac{\partial n}{\partial\vartheta}\right\rangle. \tag{65}$$

Evaluating this expression in the two opposite limits, we obtain

$$\langle\mathbf{\Gamma}_i^{\rm neo}\cdot\nabla\psi\rangle_{\rm trace}=\frac{I\langle p_z\rangle\langle\mathbf{B}\cdot\nabla\theta\rangle}{e\langle B^2\rangle}\left[\left\langle\frac{n}{b^2}\right\rangle-1+\gamma(1-\langle nb^2\rangle)\right]g \tag{66}$$

in the case of trace impurities, and

$$\langle\mathbf{\Gamma}_i^{\rm neo}\cdot\nabla\psi\rangle_{\rm Lorentz}=\frac{I\langle p_z\rangle\langle\mathbf{B}\cdot\nabla\theta\rangle}{e\langle B^2\rangle}\left[\left\langle\frac{n}{b^2}\right\rangle-\frac{1}{\langle nb^2\rangle}+\hat{\gamma}\left(1-\frac{1}{\langle nb^2\rangle}\right)\right]\hat{g}, \tag{67}$$

in the Lorentz limit. If the gradients are weak, so that g and $\hat{g}$ are both small and $n\simeq 1$, these expressions reduce to the

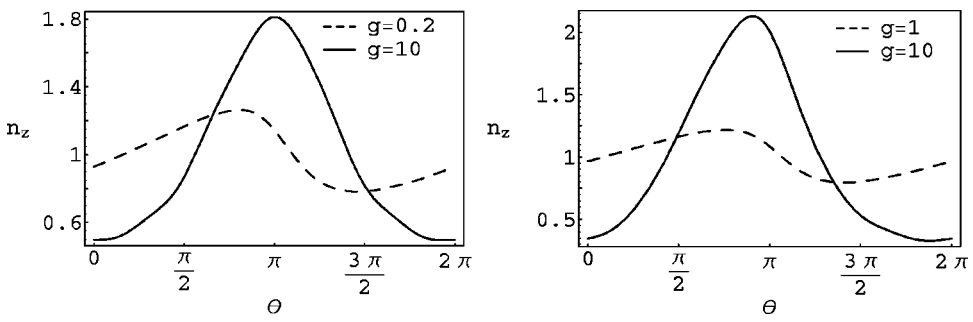

FIG. 3. Calculated impurity density vs poloidal angle θ in START at the normalized radius $r/a=0.9$; the impurity strengths are $\alpha=0.01$ and $\alpha=5$, respectively.

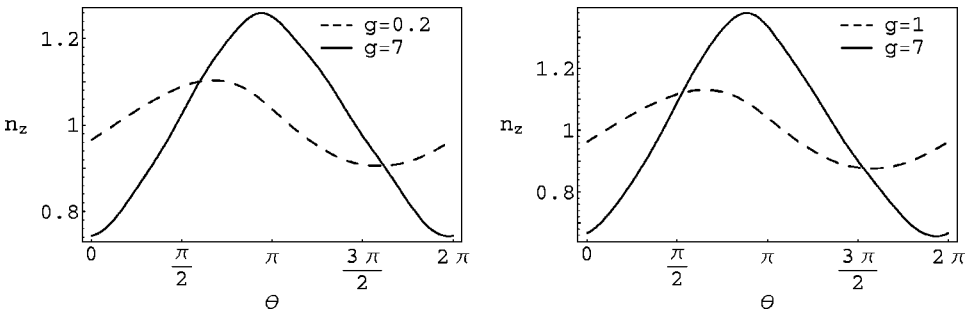

FIG. 4. Calculated poloidal variation of impurity density in the Alcator C-Mod at $r/a=0.9$ and impurity strength $\alpha=0.01$ and $\alpha=5$, respectively.

usual formula for the cross-field particle flux in the Pfirsch–Schlüter regime,[9] containing the characteristic factor $\langle b^{-2}-1\rangle$.

A. Large aspect ratio

In a plasma with small inverse aspect ratio and circular cross section, we may use the results displayed in Eqs. (61)–(64) for the impurity distribution. The particle flux then becomes

$$\langle(\mathbf{\Gamma}_i^{\mathrm{cl}}+\mathbf{\Gamma}_i^{\mathrm{neo}})\cdot\nabla\psi\rangle_{\mathrm{trace}} = \frac{\epsilon^2 p_z}{q^3 e}\left[1+\frac{2q^2}{1+g^2(1+\gamma)^2/(1+\alpha)^2}\right]g \tag{68}$$

and

$$\langle(\mathbf{\Gamma}_i^{\mathrm{cl}}+\mathbf{\Gamma}_i^{\mathrm{neo}})\cdot\nabla\psi\rangle_{\mathrm{Lorentz}} = \frac{\epsilon^2 p_z}{q^3 e}\left[1+\frac{2q^2}{1+\hat{g}^2(\hat{\gamma}-1)^2/(1+\alpha)^2}\right]\hat{g}. \tag{69}$$

In these expressions, the first term on the right is the classical flux, which is not much affected by the impurity redistribution if $\epsilon\ll 1$. The second term, which involves the Pfirsch–Schlüter factor $2q^2$, represents the neoclassical flux. This flux is suppressed if the pressure gradient becomes sufficiently steep since the denominator in the second term of Eqs. (68) and (69) depends quadratically on g and $\hat{g}$, respectively. As found earlier in the banana regime,[4,5] the classical transport then dominates, and the total flux is a nonmonotonic function of the gradients. This conclusion is thus not affected by the collisionality.

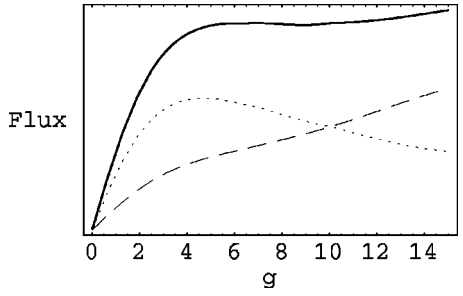

FIG. 5. Ion particle flux vs the normalized gradient g in START discharge No. 35096, in the Lorentz limit, with the impurity strength $\alpha=5$. The dashed line is the classical flux, the dotted line is the neoclassical flux, and the solid line is the sum of classical and neoclassical fluxes. The neoclassical flux is suppressed by large gradients, but the total flux is still monotonic.

In actual magnetic equilibria, the particle flux is not necessarily nonmonotonic although the neoclassical flux is suppressed when the radial pressure gradient is large. Figures 5 and 6 show particle fluxes in START and Alcator C-Mod as functions of the gradients, using the numerical solution for the impurity distribution from the previous section. Note that these particle fluxes are nonlinear but monotonic.

B. Heat flux

The heat flux can be calculated in a similar way by computing the heat friction,

$$H_{i\|}=T_i\int m_i v_\|\left(x^2-\frac{5}{2}\right)C_i(f_{i1}^0)d^3v. \tag{70}$$

In the case of trace impurities, the collision operator is dominated by ion–ion collisions, and collisions with impurities therefore hardly contribute to the heat flux. In the Lorentz limit, however, ion-impurity collisions are dominant, and the heat flux becomes

$$\langle\mathbf{q}_i^{\mathrm{neo}}\cdot\nabla\psi\rangle=-\left\langle\frac{IH_{iz\|}}{eB}\right\rangle = \chi\left[\left(\frac{d\ln p_i}{d\psi}-\frac{5}{3}\frac{d\ln T_i}{d\psi}\right)\left(\left\langle\frac{n}{b^2}\right\rangle-\frac{1}{\langle nb^2\rangle}\right) - \frac{K_z e\langle B^2\rangle}{IT_i\langle n_z\rangle}\left(\frac{1}{\langle nb^2\rangle}-1\right)\right], \tag{71}$$

where

$$\chi=\frac{45\pi}{512}\frac{I^2 p_i T_i m_i\langle n_z\rangle}{e^2\langle B^2\rangle\tau_{iz}n_z}. \tag{72}$$

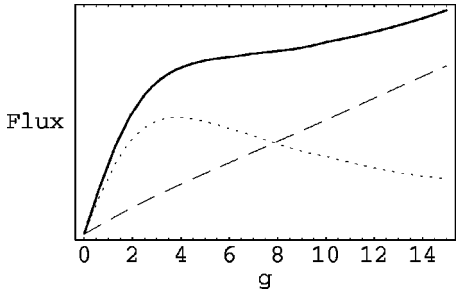

FIG. 6. The same as Fig. 5 but for Alcator C-Mod discharge No. 990920023.

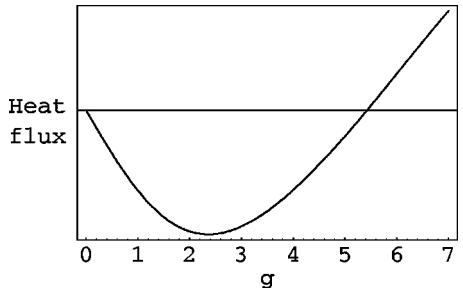

FIG. 7. Neoclassical heat flux as functions of the gradient g in a large-aspect-ratio tokamak with a circular cross section. The impurity strength is $\alpha=5$ and it was assumed that $n_i'/n_i \simeq 2T_i'/T_i$. Note the sign-reversal for large gradients.

Using Eq. (58) for K_z here gives the following result:

$$\langle \mathbf{q}_i^{\mathrm{neo}} \cdot \nabla \psi \rangle = \chi \left[\frac{d \ln p_i}{d\psi} \left(\left\langle \frac{n}{b^2} \right\rangle - 1 \right) - \frac{d \ln T_i}{d\psi} \left(\frac{5}{3} \left\langle \frac{n}{b^2} \right\rangle - \frac{8}{3\langle nb^2 \rangle} + 1 \right) \right]. \tag{73}$$

Again, in the absence of large gradients ($g \ll 1$) the impurities are evenly distributed on each flux surface ($n \to 1$), so that both terms in Eq. (71) become proportional to the Pfirsch–Schlüter factor $\langle b^{-2} - 1 \rangle$, with coefficients in agreement with Ref. 9. For large gradients ($g \gtrsim 1$), on the other hand, the poloidal redistribution of impurities affects the heat flux quantitatively and can even reverse its sign under typical conditions. Since the density profile in the tokamak edge is usually steeper than the temperature gradient, the neoclassical heat flux calculated by conventional theory is often inward. Figure 7 illustrates the neoclassical heat flux as a function of the gradients for the case where $n_i'/n_i \simeq 2T_i'/T_i$. For small radial gradients the heat flux is inward but reverses when the radial gradients become sufficiently steep. This is similar to the behavior earlier found in the banana regime.[5]

IV. CONCLUSIONS

In this paper we have investigated the character of collisional transport of an impure plasma where the pressure and temperature gradients are so large that the impurity dynamics is nonlinear. This extends earlier work, where the bulk ions were instead taken to be collisionless,[4,5] to the Pfirsch–Schlüter regime more characteristic of cool, dense plasmas. The conclusions remain broadly the same: heavy impurity ions accumulate on the inboard side of each flux surface, and this reduces neoclassical transport. In addition, they develop an up–down asymmetry, which has the same qualitative features as that measured in the Alcator C-Mod.[2] The observed asymmetry is however larger than the analytical prediction, which may have to do with the extreme steepness of the gradients in the experiments. Finally, the energy exchange between the bulk ions and electrons, which is known to significantly affect the ion heat flux in a pure plasma,[10] does not strongly influence the impurity dynamics.

ACKNOWLEDGMENTS

This work was supported by the U.K. Department of Trade and Industry, and by Euratom under association contracts with Sweden and the U.K.

[1] M. Kotschenreuther, W. Dorland, M. A. Beer, and G. W. Hammett, Phys. Plasmas **2**, 2381 (1995); A. M. Dimits, G. Bateman, M. A. Beer *et al.*, *ibid.* **7**, 969 (2000).
[2] J. E. Rice, J. L. Terry, E. S. Marmar, and F. Bombarda, Nucl. Fusion **37**, 241 (1997).
[3] T. S. Pedersen, R. S. Granetz, A. Hubbard, E. Marmar, D. Mossessian, J. Hughes, I. H. Hutchinson, J. E. Rice, and J. Terry, *Proceedings of the 27rd EPS Conference on Plasma Physics and Controlled Fusion*, Budapest, Hungary, 12–16 June 2000, edited by K. Szegö, T. N. Todd, and S. Zoletnik (European Physical Society, Geneva, 2000).
[4] P. Helander, Phys. Plasmas **5**, 3999 (1998).
[5] T. Fülöp and P. Helander, Phys. Plasmas **6**, 3066 (1999).
[6] C. T. Hsu and D. J. Sigmar, Plasma Phys. Controlled Fusion **32**, 499 (1990).
[7] F. L. Hinton and R. D. Hazeltine, Rev. Mod. Phys. **48**, 239 (1976).
[8] S. P. Hirshman and D. J. Sigmar, Nucl. Fusion **21**, 1079 (1981).
[9] P. H. Rutherford, Phys. Fluids **17**, 1782 (1974).
[10] F. Engelmann and A. Nocentini, Nucl. Fusion **17**, 995 (1977).
[11] K. H. Burrell and S. K. Wong, Nucl. Fusion **19**, 1571 (1979).
[12] M. Tendler, in *Plasma Physics and Controlled Fusion Research*, Proceedings of the 8th International Conference on Plasma Physics and Controlled Fusion Research, Brussels (International Atomic Energy Agency, Vienna, 1981), Vol. 1, p. 765.
[13] H. A. Claassen, H. Gerhauser, A. Rogister, and C. Yarim, Phys. Plasmas **7**, 3699 (2000).
[14] R. D. Hazeltine, Phys. Fluids **17**, 961 (1974).
[15] M. Gryaznevich, R. Akers, P. G. Carolan *et al.*, Phys. Rev. Lett. **80**, 3972 (1998).